

Multistatic Tracking for Continuous Active Sonar using Doppler-Bearing Measurements

Doug Grimmett, Cherry Wakayama

Maritime Systems Division – Code 56490

SPAWAR Systems Center Pacific

San Diego, CA, U.S.A.

grimmett@spawar.navy.mil, cherry.wakayama@navy.mil

Abstract—Unlike conventional Pulsed Active Sonar (PAS) which listens for echoes in between short-burst transmissions, Continuous Active Sonar (CAS) attempts to detect echoes amidst the continual interference from source(s) transmitting with nearly 100% duty cycle. The potential advantage of CAS is an increased number of continuous detection opportunities, leading to improved target detection, localization, tracking, and classification. The challenge is detecting the target echoes in the presence of continuous interference. CAS transmission waveforms may be of several types, i.e., frequency modulated waveforms (FMs) which provide good range measurements, continuous waveforms (CWs) which provide good Doppler measurements, or sophisticated broadband waveforms which attempt to provide both good range and Doppler measurements simultaneously. In order to mitigate against the multi-source mutual interference problem, it may be preferred to only use continuous CW transmissions, rather than continuously repeating broadband waveforms. This paper develops a tracking approach based on the Gaussian Mixture Probability Hypothesis Density (GMPHD) filter for multistatic sonar configurations using Doppler-bearing measurements from continuous CW transmissions. From a single fixed source-receiver node, such measurements do not enable precise target state estimates. However, when data fusion and target tracking is performed amongst multiple source-receiver nodes, it is shown that good localization estimates and target tracking may be obtained.

Keywords—Continuous Active Sonar; multistatic tracking; GMPHD; Doppler-bearing tracking

I. INTRODUCTION

Distributed multistatic active sonar networks have the potential to increase ASW performance against small, quiet, threat submarines in the harsh, clutter-saturated littoral and deeper ocean environments. This improved performance comes through the expanded geometric diversity of a distributed field of sources and receivers and results in increased probability of detection, area coverage, target tracking, classification, and localization [1].

Recently, there has been renewed interest in the concept of Continuous Active Sonar (CAS). Unlike Pulsed Active Sonar (PAS) which listens for echoes in between short transmission bursts, CAS attempts to detect echoes amidst the continual interference from source(s) transmitting with nearly 100% duty cycle. A schematic of the two contrasting approaches is shown in Fig. 1. The potential advantage of CAS is an increased

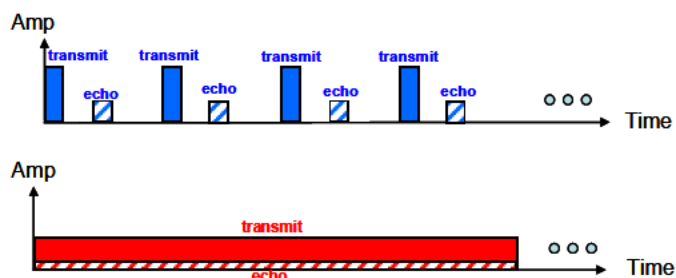


Fig. 1. Depiction of PAS (top, blue) and CAS (bottom, red) methods. The PAS “listens after transmit” and the CAS method “listens while transmit”.

number of continuous detection opportunities, leading to improved target detection, localization, tracking, and classification. In addition, lower transmission source levels are possible. Of course, appropriate CAS-specific processing must be employed to enable detection in the presence of continuous transmissions.

Employing the CAS concept for multistatic active sonobuoy fields presents additional challenges beyond what is the case for surface ship sonar implementations which are typically employed in monostatic (single source and receiver) configurations. The primary challenge for multistatic sonobuoy systems is that they may have less bandwidth available for use, and therefore, multiple CAS sources may transmit and interfere with one another in the same frequency band, at the same time. In addition, transmission source level and operational duration are limited by available battery energy of the sonobuoys. Finally, buoy positions may be less accurately known. Despite these difficulties, there is potential to increase performance through the increased number of detections available through the CAS processing and the fusion of multiple sensors within the field.

Like PAS systems, CAS systems may employ a variety of signal types; amongst the most common are: FM, CW, and more advanced signals which attempt to capture the advantages of both FM and CW waveforms simultaneously. FM waveforms provide good ranging information whereas CW waveforms provide good Doppler (range-rate) information. When bandwidth is very limited and multi-source interference

Report Documentation Page

Form Approved
OMB No. 0704-0188

Public reporting burden for the collection of information is estimated to average 1 hour per response, including the time for reviewing instructions, searching existing data sources, gathering and maintaining the data needed, and completing and reviewing the collection of information. Send comments regarding this burden estimate or any other aspect of this collection of information, including suggestions for reducing this burden, to Washington Headquarters Services, Directorate for Information Operations and Reports, 1215 Jefferson Davis Highway, Suite 1204, Arlington VA 22202-4302. Respondents should be aware that notwithstanding any other provision of law, no person shall be subject to a penalty for failing to comply with a collection of information if it does not display a currently valid OMB control number.

1. REPORT DATE

JUN 2013

2. REPORT TYPE

3. DATES COVERED

00-00-2013 to 00-00-2013

4. TITLE AND SUBTITLE

Multistatic Tracking for Continuous Active Sonar using Doppler-Bearing Measurements

5a. CONTRACT NUMBER

5b. GRANT NUMBER

5c. PROGRAM ELEMENT NUMBER

6. AUTHOR(S)

5d. PROJECT NUMBER

5e. TASK NUMBER

5f. WORK UNIT NUMBER

7. PERFORMING ORGANIZATION NAME(S) AND ADDRESS(ES)

SPAWAR Systems Center Pacific, Maritime Systems Division ? Code 56490, San Diego, CA, 92152

8. PERFORMING ORGANIZATION REPORT NUMBER

9. SPONSORING/MONITORING AGENCY NAME(S) AND ADDRESS(ES)

10. SPONSOR/MONITOR'S ACRONYM(S)

11. SPONSOR/MONITOR'S REPORT NUMBER(S)

12. DISTRIBUTION/AVAILABILITY STATEMENT

Approved for public release; distribution unlimited

13. SUPPLEMENTARY NOTES

Presented at the 16th International Conference on Information Fusion held in Istanbul, Turkey on 9-12 July 2013. Sponsored in part by Office of Naval Research Global.

14. ABSTRACT

Unlike conventional Pulsed Active Sonar (PAS) which listens for echoes in between short-burst transmissions Continuous Active Sonar (CAS) attempts to detect echoes amidst the continual interference from source(s) transmitting with nearly 100% duty cycle. The potential advantage of CAS is an increased number of continuous detection opportunities, leading to improved target detection, localization, tracking, and classification. The challenge is detecting the target echoes in the presence of continuous interference. CAS transmission waveforms may be of several types, i.e., frequency modulated waveforms (FMs) which provide good range measurements continuous waveforms (CWs) which provide good Doppler measurements, or sophisticated broadband waveforms which attempt to provide both good range and Doppler measurements simultaneously. In order to mitigate against the multi-source mutual interference problem, it may be preferred to only use continuous CW transmissions, rather than continuously repeating broadband waveforms. This paper develops a tracking approach based on the Gaussian Mixture Probability Hypothesis Density (GMPHD) filter for multistatic sonar configurations using Doppler-bearing measurements from continuous CW transmissions. From a single fixed source-receiver node, such measurements do not enable precise target state estimates. However, when data fusion and target tracking is performed amongst multiple source-receiver nodes, it is shown that good localization estimates and target tracking may be obtained.

15. SUBJECT TERMS

16. SECURITY CLASSIFICATION OF:			17. LIMITATION OF ABSTRACT Same as Report (SAR)	18. NUMBER OF PAGES 8	19a. NAME OF RESPONSIBLE PERSON
a REPORT unclassified	b ABSTRACT unclassified	c THIS PAGE unclassified			

Standard Form 298 (Rev. 8-98)
Prescribed by ANSI Std Z39-18

is possible (e.g. multistatic operations), it may be preferable to use only continuous CW transmissions, rather than continuously repeating broadband waveforms such as FM. With CWs it may be easier to mitigate the mutual interference of multi-source operations.

This paper explores a multistatic CAS configuration using CW waveforms, which provide measurements of target Doppler and target bearing. From a single fixed source-receiver node, such measurements do not enable precise target localization. However, when data fusion and target tracking is performed amongst multiple source-receiver nodes, good localization estimates and target tracking may be obtained. The tracking approach presented here is based on the Gaussian Mixture Probability Hypothesis Density (GMPHD) filter.

Further description and processing methods for CAS are described in Section II. Section III describes the GMPHD tracking approach for the Doppler-bearing measurements of a multistatic CW CAS system. The simulation which provided contact-level CAS data for our analysis is described in Section IV. Section V provides the GMPHD tracking results, and Section VI provides a summary.

II. CONTINUOUS ACTIVE SONAR

A description and comparison of two basic CAS modes, FM and CW, is given. We assume a system in which receivers perform beamforming or adaptive beamforming to obtain bearing estimates of target echoes as well as to suppress the direct blast interference coming from the source(s).

A. CAS FM mode

The use of a repeating linear FM (LFM) signal in CAS provides the ability obtain range estimates of detected targets by measuring echo time delays. Fig. 2 shows an LFM waveform with total bandwidth, B , and the same duration as its ping repetition interval, T_{PRI} . The echo from a target arrives with time delay, $\Delta\tau$, which may be obtained by temporal processing; i.e., matched filtering of the data with a sub-replica of specified bandwidth B_P . Continuous processing may be achieved by splitting the total signal bandwidth into a number of frequency sub-bands and processing with a bank of matched filters.

Alternatively, the time delay may be obtained by performing spectral processing. Using the Short Time Fourier Transform (STFT), the frequency shift, Δf , may be obtained, and from this, the time delay is determined using the relationship:

$$\Delta\tau = \Delta f \cdot \frac{T_{PRI}}{B} \quad (1)$$

Continuous processing is achieved by repeating the STFT and producing spectrogram output. A target with Doppler (range-rate) may induce some bias error into the range measurement, according to the ambiguity function of the sub-section of LFM signal processed [2]. In practice, the spectral processing method is most conveniently achieved by heterodyning (de-chirping) the received signal by the transmitted signal [3-4], prior to spectrogram processing.

Fig. 3 shows an example of the potential challenge of mutual interference (as seen by a receiver) when multiple sources in the field utilize the same waveform or frequency band. In this example we show three LFM waveforms, all with the same T_{PRI} and bandwidth; two are upsweeps and one is a downsweep. It is clear that the potential for interference is significant, with multiple direct transmissions and echoes contained in each processing block. Such interference may be mitigated through the use of more sophisticated wideband waveforms (such as those with orthogonal properties) and advanced processing techniques [5].

B. CAS CW mode

The use of a continuous CW signal in CAS provides the ability to obtain continual range-rate estimates of detected targets by measuring Doppler shifts. Fig. 4 shows such a CW signal transmission. The echo from a target arrives with time delay, $\Delta\tau$, but this (and hence range) is not measurable and therefore indiscernible using this method. However the target Doppler

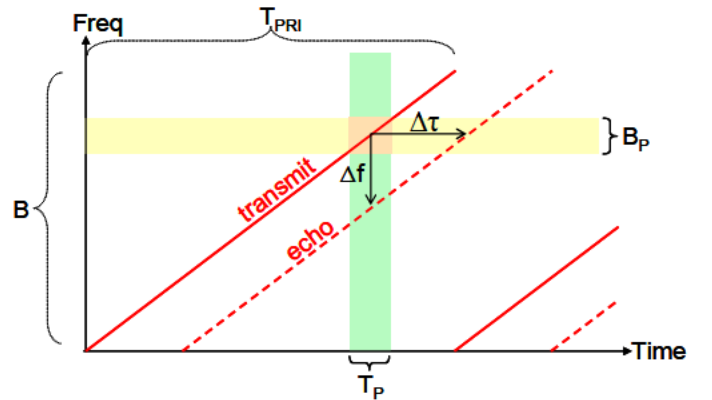


Fig. 2. Depiction of CAS LFM mode. Yellow indicates the temporal processing method and the green indicates the spectral processing method.

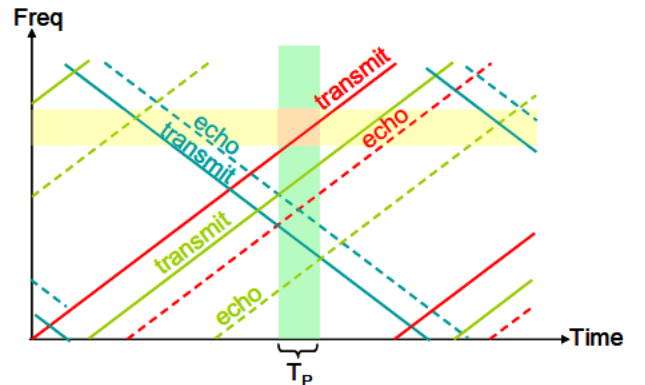


Fig. 3. Depiction of the mutual interference challenge of multi-source CAS FM mode (3 sources) at a receiver; two LFM upsweeps and one LFM downsweep occupying the same frequency band (and with the same repetition cycle).

shift, Δf , is measurable, provided that it is sufficiently separated from the transmitted signal and louder than the reverberation/noise background. Continuous measurements are obtainable through spectral processing (STFT/spectrogram). This measured Doppler shift corresponds to the target's bistatic range-rate [6], which can be used in multistatic fusion and tracking algorithms.

Whereas the CAS LFM mode shows significant potential for multi-source mutual interference, CAS CW mode may be configured in a way to avoid this problem. This is done simply by allocating a separate sub-band of the overall available frequency band to each source, as indicated in Fig. 5. Each sub-band needs only enough bandwidth to unambiguously accommodate the maximum expected (opening and closing) Doppler shifts of targets. Done this way, there is no cross-interference between multiple sources at any receiver. Although such Doppler measurements don't localize the target as quickly or precisely as ranging measurements (obtainable with FM waveforms) do, with an effective multistatic data fusion process, good target tracking may be achieved.

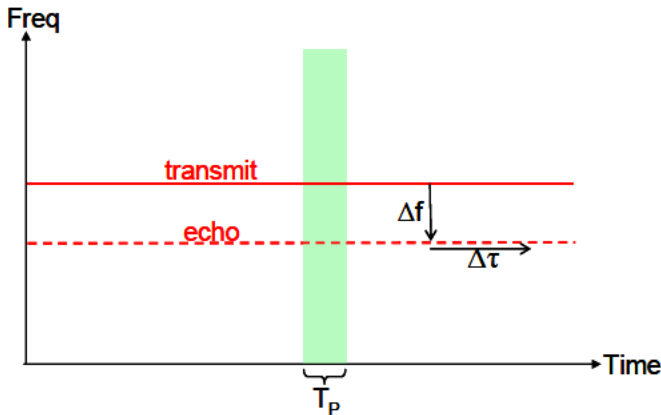


Fig. 4. Depiction of the CAS CW mode.

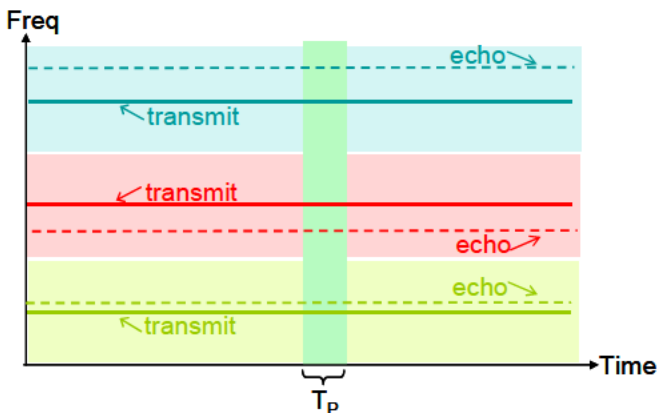


Fig. 5. Mutual interference mitigation using frequency sub-band allocation (blue/red/green) for each source and using CW waveforms.

III. GAUSSIAN MIXTURE PROBABILITY HYPOTHESIS DENSITY (GMPHD) TRACKER

Because of the nature of CW CAS signals, target range is not directly measurable. Obtaining target state (localization) estimates using only bearing and Doppler measurements can be problematic. A single bearing-Doppler measurement from a target received by a single source-receiver pair has limited observability, i.e., the target's state vector (position and speed) is ambiguous. Normally, additional measurements are needed to resolve this ambiguity, which may be obtained over time. However, to completely disambiguate and localize the target state, motion of the source-receiver pair is required, as is the case with passive bearings-only Target Motion Analysis (TMA) methods [7]. However, in our case, the sensors are assumed to be relatively stationary and therefore we are unable to employ such localization methods. Instead, we must estimate the target state using other methods. Methods for target tracking using fixed-sensor passive bearings-only measurements to cue active multistatic tracking have been developed [8-9]. These approaches assume fixed receivers and use Gaussian Mixtures (GM) and a bank of Kalman filters to deal with localization ambiguity. Other approaches have addressed the multistatic Doppler-only measurement (no bearings) case with GMPHD [10] and with a Likelihood ratio tracker [11]. Unlike those approaches, here we wish to take advantage of the availability of active Doppler measurements in addition to bearing measurements to improve target tracking through multi-sensor fusion.

Because of the lack of observability with individual measurements, we choose here to investigate the potential of multi-sensor fusion methods which can provide good target localization and tracking. For this paper, we have chosen to utilize the Gaussian Mixture Probability Hypothesis Density (GMPHD) filter. The GMPHD filter is a relatively recent development and shows good potential in addressing the multiple-target, multiple-detection association problem. It outputs a posterior intensity surface from which the target localization can eventually be estimated. There may be other approaches that could equivalently be employed, such as the Likelihood Ratio Tracker (LRT) surface [12], the Hybrid Intensity Likelihood Ratio Tracker (iLRT) [13], or others. The objective of this paper is to demonstrate the potential of successful target tracking using the Doppler-bearing measurements of CW CAS, as well as the improvement expected when multi-sensor fusion is employed. A specific algorithm recommendation, whether the GMPHD filter or one of its alternatives, is not the focus of this paper.

A. Sensor and Measurement Model

We consider that a target is described by its state vector

$$X = [x, y, \dot{x}, \dot{y}]^T \quad (2)$$

where x, y, \dot{x}, \dot{y} represent 2-dimensional positions and velocities. The target motion is modeled with the well known *nearly constant velocity* (NCV) motion model [14]. CAS CW processing yields measurements of bearing, θ , and bistatic range-rate, \tilde{r} , which is obtained from the observed Doppler shift, Δf , as

$$\tilde{r} = -\frac{\Delta f}{2f_0}c \quad (3)$$

where f_0 is the transmitted frequency and c is the speed of sound in water. The measurements of bearing and range-rate are non-linear functions of the target state, X , with measurement noise, as follows:

$$Z = \begin{bmatrix} \theta \\ \tilde{r} \end{bmatrix} = \begin{bmatrix} h_1(X) \\ h_2(X) \end{bmatrix} + v, \quad (4)$$

$$v \sim N(0, R), \quad \text{with} \quad R = \begin{bmatrix} \sigma_\theta^2 & \sigma_{\theta\tilde{r}} \\ \sigma_{\theta\tilde{r}} & \sigma_{\tilde{r}}^2 \end{bmatrix}. \quad (5)$$

The non-linear measurement functions for bearing and range-rate are given as follows:

$$h_1(X) = \tan^{-1}\left(\frac{y - y^R}{x - x^R}\right) \quad (6)$$

$$h_2(X) = \frac{\begin{bmatrix} \dot{x} - \dot{x}^S \\ \dot{y} - \dot{y}^S \end{bmatrix}^T \cdot \begin{bmatrix} x - x^S \\ y - y^S \end{bmatrix}}{2r_{TS}} + \frac{\begin{bmatrix} \dot{x} - \dot{x}^R \\ \dot{y} - \dot{y}^R \end{bmatrix}^T \cdot \begin{bmatrix} x - x^R \\ y - y^R \end{bmatrix}}{2r_{TR}} \quad (7)$$

where

$$r_{TS} = \left\| \begin{bmatrix} x - x^S \\ y - y^S \end{bmatrix} \right\|, \quad r_{TR} = \left\| \begin{bmatrix} x - x^R \\ y - y^R \end{bmatrix} \right\|, \quad (8)$$

and where the source and receiver states are given by $[x^S, y^S, \dot{x}^S, \dot{y}^S]^T$ and $[x^R, y^R, \dot{x}^R, \dot{y}^R]^T$, respectively. The Jacobian provides the linearization to be used in the Extended Kalman Filter (EKF) formulation, and the measurement matrix is given by

$$H = \begin{bmatrix} H_{11} & H_{12} & H_{13} & H_{14} \\ H_{21} & H_{22} & H_{23} & H_{24} \end{bmatrix} \quad (9)$$

where

$$H_{11} = \frac{\partial h_1(X)}{\partial x} = \frac{-(y - y^R)}{(x - x^R)^2 + (y - y^R)^2} \quad (10)$$

$$H_{12} = \frac{\partial h_1(X)}{\partial y} = \frac{(x - x^R)}{(x - x^R)^2 + (y - y^R)^2} \quad (11)$$

$$H_{13} = \frac{\partial h_1(X)}{\partial \dot{x}} = 0 \quad (12)$$

$$H_{14} = \frac{\partial h_1(X)}{\partial \dot{y}} = 0 \quad (13)$$

and

$$H_{21} = \frac{\partial h_2(X)}{\partial x} = \frac{(y - y^S)^2(\dot{x} - \dot{x}^S) - (x - x^S)(y - y^S)(\dot{y} - \dot{y}^S)}{2r_{TS}^3} + \frac{(y - y^R)^2(\dot{x} - \dot{x}^R) - (x - x^R)(y - y^R)(\dot{y} - \dot{y}^R)}{2r_{TR}^3} \quad (14)$$

$$H_{22} = \frac{\partial h_2(X)}{\partial y} = \frac{(x - x^S)^2(\dot{y} - \dot{y}^S) - (x - x^S)(y - y^S)(\dot{x} - \dot{x}^S)}{2r_{TS}^3} + \frac{(x - x^R)^2(\dot{y} - \dot{y}^R) - (x - x^R)(y - y^R)(\dot{x} - \dot{x}^R)}{2r_{TR}^3} \quad (15)$$

$$H_{23} = \frac{\partial h_2(X)}{\partial \dot{x}} = \frac{(x - x^S)}{2r_{TS}} + \frac{(x - x^R)}{2r_{TR}} \quad (16)$$

$$H_{24} = \frac{\partial h_2(X)}{\partial \dot{y}} = \frac{(y - y^S)}{2r_{TS}} + \frac{(y - y^R)}{2r_{TR}}. \quad (17)$$

B. GMPHD filter

The Probability Hypothesis Density (PHD) tracking approach [15] is a Bayesian filtering formulation which utilizes Random Finite Sets (RFS). The collection of individual targets is treated as a set-valued state and the collection of individual observations is treated as a set-valued observation. The PHD filter propagates only the first-order statistical moment (i.e. intensity) of the RFS states in time, and thereby avoids the combinatorial problem of data association. However, the PHD recursion for this filter has no closed form solution, making its implementation difficult.

The multi-target GMPHD filter provides an analytic solution to the PHD recursion for linear Gaussian target dynamics and Gaussian birth model [16]. It uses the convenient form of Gaussian Mixtures (GM) for the prior and posterior PHD intensities, and provides closed form recursions for GM weights, means, and covariances. Non-linear measurement models may be also incorporated using Extended Kalman filter (EKF) and Unscented Kalman filter (UKF) formulations. In this paper we implemented an EKF version of GMPHD and applied it to a simulated CAS data set. Details of the approach, including the relevant equations and pseudo-code are found in [16]. Our sensor and measurement model was described in the previous section.

A brief summary of our implementation of the GMPHD filter follows:

- New target intensity is injected into the filter each processing interval. In our case, this consists only of a target birth process; no target spawning is considered. The birth intensity that is added is provided by a set of GM components whose mean locations are uniformly distributed over the desired surveillance space. Each component's covariance is appropriately scaled to provide continuous coverage.
- Predictions for all the GM components representing existing and new targets are performed using a standard *nearly-constant-velocity* motion model.
- The PHD update is performed using all of the incoming measurements for a given processing scan. An extended Kalman filter update is made between each of the predicted GM components and the new measurements. The posterior intensity is represented by a GM which has an increased number of components.

- All posterior GM components with low weight (below a threshold) are eliminated. All GM components that are in close proximity to each other (within a threshold) are merged. GM components with weights above a threshold are reported out and provided to a post-processing data association filter.
- New contact data is accumulated and the procedure iterates.

C. Post-GMPHD Data Association for Output Tracks

The GMPHD filter estimates multi-target states by determining the Gaussian components within the intensity surface which have high weight (above a suitable threshold). They provide estimates of the target states over time. However, the GMPHD output does not perform any association of these extracted state estimates over time to create and identify specific target tracks.

In [17] a multiple hypothesis tracking (MHT) based data association filter to extract tracks from the GMPHD output is described. Here we have applied a linear Kalman-based, global nearest neighbor (GNN) data association filter to the extracted GMPHD state estimates (those with weights that exceed a threshold). The GNN filter determines the most likely global GMPHD estimate-to-track association from scan-to-scan and outputs track estimates over time. This step ensures that GMPHD outputs are associable and provides a more conventional tracker display which is convenient for sonar operators.

IV. MULTISTATIC CAS SIMULATION

A simulation was made of a CAS scenario to provide *contact-level* data for testing the GMPHD tracking and fusion algorithm. The scenario is depicted in Fig. 6. There are three acoustic sources separated by 5 km in a north-south orientation; three planar receive (hydrophone) arrays are collocated with the sources. A target approaches the field with a heading of 90° (clockwise from North) and speed of 5 kts. Each source is assumed to transmit continuous CW waveforms in non-overlapping frequency bands to avoid mutual interference between them and allow the possibility of simultaneous detections from each source (e.g. see Fig. 5). The duration of this scenario is assumed to be 365 seconds.

The assumed receiver processing chain is now described. Each receiver acquires hydrophone signals, which are composed of the direct-blast energy, potential target and false alarm echoes, acoustic reverberation, and ambient noise. These signals are then processed to provide a set of beams, which provide (azimuthal) bearing measurements of the received acoustic energy. A Spectrogram of each beam is then produced by taking the STFT, over successive processing intervals, T_p , which we assumed to be 5 seconds. Each STFT output is normalized across frequency and when the acoustic power exceeds a threshold, detection echoes (contacts) are extracted. The Doppler shift (from the transmitted CW) corresponds to a bistatic range-rate according to Eq. (3). The resulting *contact-level* data are a set of measurements which include: time, bearing, and bistatic range-rate. The CAS

simulation does not actually implement the aforementioned signal processing chain, but instead directly simulates the contact-level data resulting from such processing. Each receiver can process each source signal, so there are 9 possible detection opportunities per processing interval (three monostatic and 6 bistatic). A *scan* is defined as the output of a single processing interval for a source-receiver pair (one frequency). There are nine scans available per processing interval and a total of 657 scans collected over the duration of the entire scenario.

The target-originated contacts were generated as follows. The active sonar equation is modeled using the Passive-Active Contact Simulator (PACsim) [18]. Outputs are obtained for each source-target-receiver geometry, for every scan. PACsim includes acoustic modeling of transmission loss, reverberation, and noise. It also includes modeling of the sonar system, including spatial and temporal processing gains and detection processes. An aspect-dependent, bistatic TS model is used. A suitable Doppler detection model is implemented.

PACsim calculates mean signal excess \overline{SE} (in dB) for each target echo. Because of the uncertainties in the sonar equation and expected real-world fluctuations, variations from the mean levels are expected. In our case we assume them to be normally distributed as: $SE = \overline{SE} + \xi$, where $\xi \sim N(0, \sigma_{SE})$; we assume $\sigma_{SE} = 10$ dB. Measurements of bearing and Doppler are computed from the true geometry, but with random errors added. These are sampled from normal distributions with standard deviations of $\sigma_\theta = 3^\circ$ and $\sigma_f = 0.1$ m/s.

False alarms were also simulated by randomly generating additional detection contacts within each processing scan. The false alarms are distributed uniformly across all possible bearing and Doppler limits of the system. The number and amplitudes (SNRs) of the false alarms is user-controllable. In our case the number of false alarms injected was approximately four per scan.

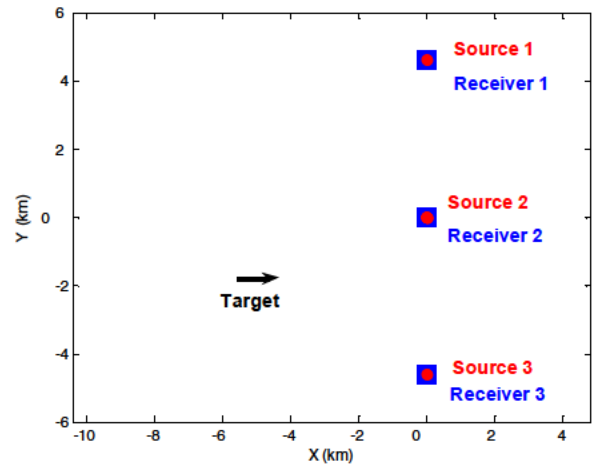


Fig. 6. CW CAS simulation scenario. Sources (red dots), receivers (blue squares), and target trajectory (black).

V. MULTISTATIC TRACKING RESULTS

The GMPHD tracking filter was applied to the simulated scenario previously described. Four cases of data fusion with increasing complexity were considered as follows:

- Case 1. Monostatic– Source 2 with Receiver 2, one scan per processing interval
- Case 2. Multi-Source– Sources 1,2,3 with Receiver 2, three scans per processing interval
- Case 3. Multi-Receiver– Source 2 with Receivers 1,2,3, three scans per processing interval
- Case 4. Multistatic– Sources 1,2,3 with Receivers 1,2,3, nine scans per processing interval

Case 1 processes one scan per processing interval, cases 2 and 3 process three scans per interval, and case 4 processes nine scans per interval. In each case, the GMPHD tracker was applied with parameters set to the values listed in Table I.

Fig. 7 shows the GMPHD output intensity surface for the positional portion of the target state, obtained after the first processing interval. We see that the single-node case 1 shows only a broad area of weak intensity with no prominent peaks. Case 2 shows more intensity has built up, due to the increased data being fused from the three sources. However, there are still no prominent peaks near the target value at this early stage. Case 3 shows a very discernable intensity peak, which is obtained through the cross-fixing effect of fusing the three receivers. However, it is not aligned very well with the true target value. Finally, when all the nine nodes are fused in case 4, the intensity surface shows a strong peak at the correct location. The advantage of sensor fusion is apparent even though very few measurements have been processed.

Fig. 8 shows the GMPHD positional intensity after about 220 seconds (2/3 the way through the scenario). Compared to Fig. 7, here we see nice strong intensity peaks have built up over time and good localization is achieved, particularly for cases 2-4. We observe that case 4 has the highest intensity peak and most accurate localization due to full field fusion.

TABLE I. GMPHD PARAMETERS.

Parameter Description	Value
Bearing error, σ_θ	3
Rate-rate error, σ_r	0.1 m/s
Error correlation, $\sigma_{\theta r}$	0 deg·m/s
Motion model process noise q_x, q_y	0.01 m ² /s ³
Probability of target death	0.001
Probability of detection	0.95
Clutter rate (per scan)	5
Extraction threshold	2.5
# Gaussian birth terms	100
GM component elimination threshold	1e-12
GM component merge threshold	4
Surveillance area	X=-(6 to 4) km Y = -(3 to 1) km

Case 3 also shows a strong peak but it is slightly biased in its position relative to case 4. It is also stronger than the intensity seen in case 2.

Fig. 9 shows the GMPHD intensity surface for the velocity portion of the target state, obtained after the first processing interval. We see that cases 1-3 all show an ambiguity ridge for the estimated velocity of the target, though cases 2-3 are better than case 1. The full-field fusion of case 4 shows an excellent estimation result for the target velocity. Fig. 10 shows the velocity intensity after about 220 seconds (2/3 the way through the scenario), corresponding to Fig. 8. Here we see that while ambiguity still exists in the single-node of case 1, cases 2-3

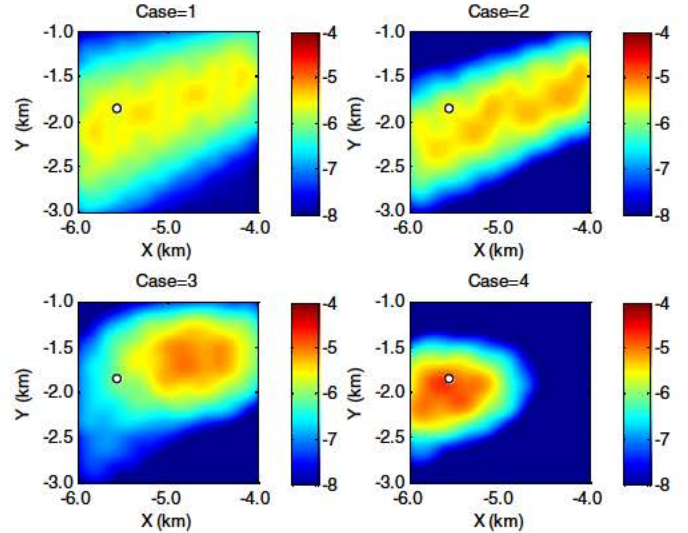


Fig. 7. GMPHD positional intensity over the target surveillance region after completion of the first processing interval. White marker is the true target value and each case has the same colorscale (log of intensity).

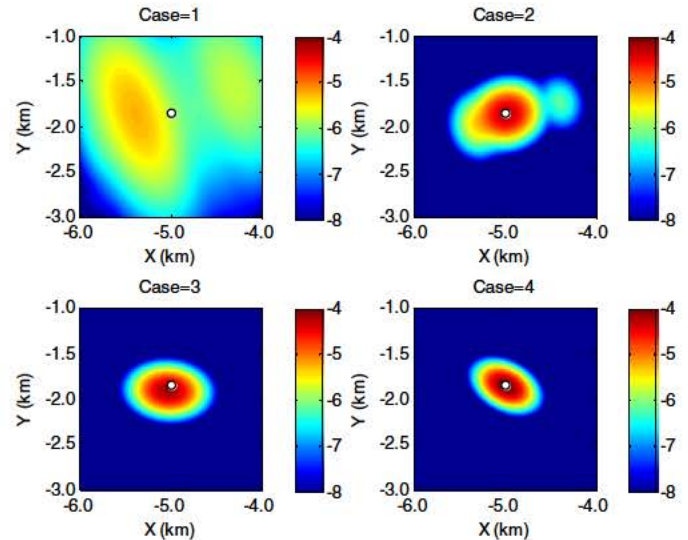


Fig. 8. GMPHD positional intensity over target surveillance region after 220 seconds (2/3 the way through scenario). White marker is the true target value, and each case has the same colorscale (log of intensity).

show good target velocity estimate after this much time. Case 4 shows a very precise estimate of the target velocity.

The output of the GMPHD filter was input into the GNN data association filter for final tracker output. Fig. 11 is the cumulative tracker output for case 1 over the entire scenario. It shows a few extracted detections which give rise to a short-lived, somewhat inaccurate target track estimate. There are also a couple of false target tracks which arise due to the false alarm clutter which is present in the data.

Fig. 12 shows the results of the tracker for case 2, with the fusion of detections from all three sources. We observe that in contrast to the processing of a single node, the fusion of data

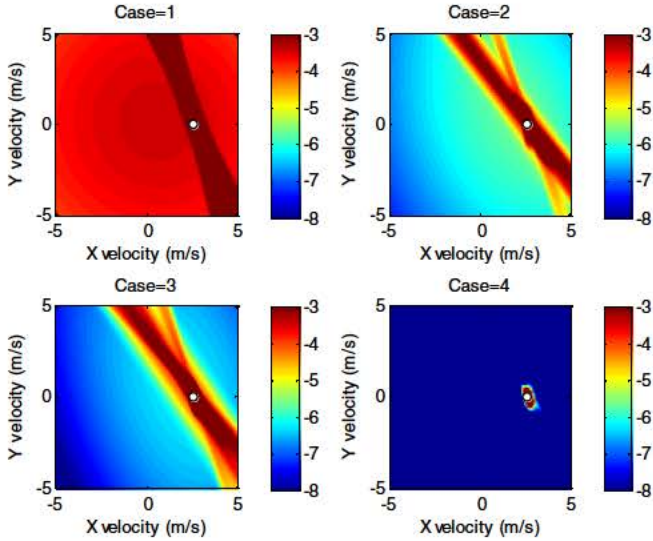


Fig. 9. GMPHD velocity intensity surface after the first processing interval. Colorscale is log of intensity and white marker is the true target value.

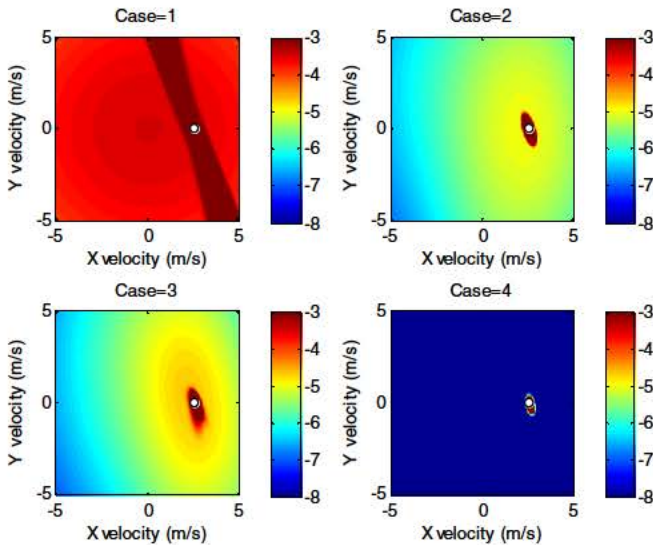


Fig. 10. GMPHD velocity intensity surface after 220 seconds into the scenario (2/3 the way complete). Colorscale is log of intensity and white marker is the true target value.

from the multiple sources provides accurate target tracking on the latter half of the target's trajectory. There are also two false tracks which occur at similar bearings (but closer range) from receiver 2.

Fig. 13 shows the output of the tracker for source 2 with detections from all three receivers (case 3). The tracker output is much improved over the previous cases, with longer hold time on the target and no false tracks. The improved performance seen here can be attributed to the geographic diversity provided by spatially distributed receivers. Each receiver sees the target from a different vantage point and the intersecting detection bearings provide a better and earlier target cross-fix within the GMPHD filter (as in Fig. 7). We observe startup effect at the beginning of the track as the GMPHD filter is converging on the actual target. There is also a slight southerly localization bias of the track estimate.

Fig. 14 shows the output of the tracker with the fusion the all sources and all receivers. The tracker output is further improved, and has the longest target hold time and localization accuracy of all the cases considered. There were no false tracks. The benefit of multi-sensor fusion is clearly demonstrated with these results.

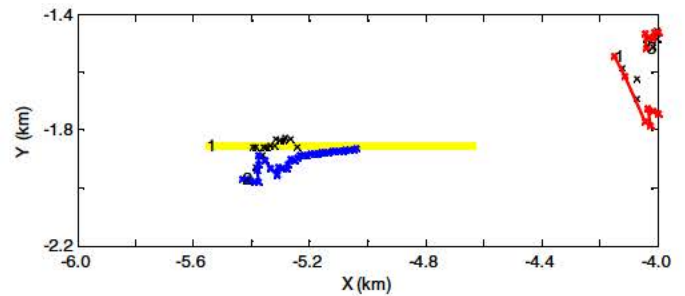


Fig. 11. Tracker output case 1 (monostatic); target true trajectory (yellow), GMPHD output (black); target track (blue), false tracks (red).

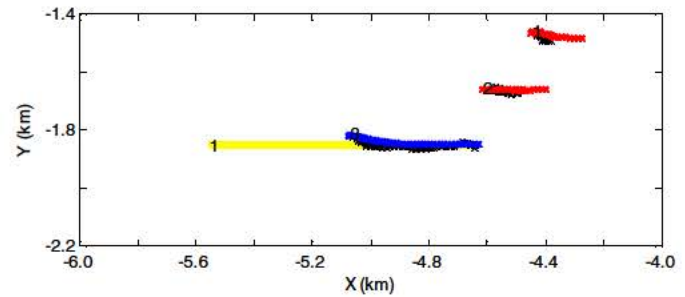


Fig. 12. Tracker output case 2 (multi-source); target true trajectory (yellow), GMPHD output (black); target track (blue), false tracks (red).

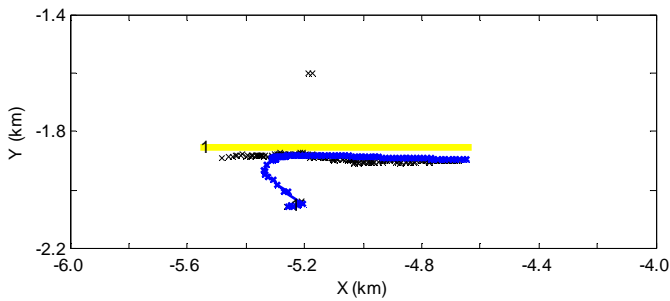


Fig. 13. Tracker output case 3 (multi-receiver); target true trajectory (yellow), GMPHD output (black); target track (blue).

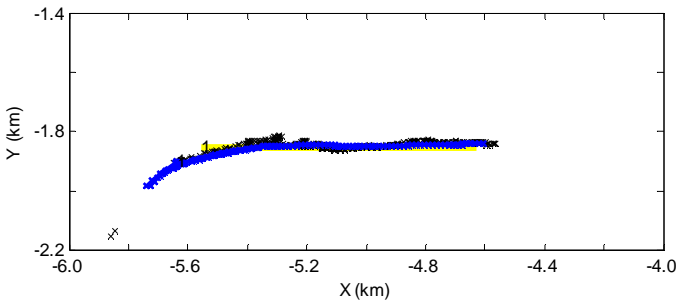


Fig. 14. Tracker output case 4 (multistatic); target true trajectory (yellow), GMPHD output (black); target track (blue).

VI. SUMMARY

A potential operating mode for CAS with CW transmissions in multistatic configurations has been presented. The advantage of this approach is that the multisource interference issue within a multistatic operation can easily be mitigated. Though target ranging measurements are not available in this configuration, it has been shown that good target tracking and localization can nevertheless be obtained through an effective fusion of multiple sensors with Doppler-bearing measurements. This was done using an Extended Kalman Filter implementation of the GMPHD filter. The results show that using only a single (monostatic) sonar node was much less effective in tracking the target than when cross-sensor fusion was applied. In general, the results show that fusion of multiple receivers (with a single source) will perform better than fusion of multiple sources (with a single receiver). This is due to the positional localization improvement available when multiple target bearings are cross-fixed. Further improved results are obtained when all the available (and detecting) nodes are included in the fusion processing.

REFERENCES

- [1] D. Grimmer and S. Coraluppi, Multistatic active sonar system interoperability, data fusion, and measures of performance, *NURC Technical Report NURC-FR-2006-004*, April 2006 [NATO UNCLASSIFIED releasable for internet transmission].
- [2] X. Song, P. Willet, S. Zhou, Posterior Cramer-Rao Bounds for Doppler biased Multistatic Range-only Tracking, in *proceedings 14th International Conference on Information Fusion*, Chicago, U.S.A., July 2011.
- [3] A. A. Winder, "II. Sonar System Technology", *IEEE Trans. Sonics and Ultrasonics*, Vol SU-22, No. 5, September 1975.
- [4] B. Siciliano, K. Oussama, Eds., "Springer Handbook of Robotics", Springer: Verlag Berlin Heidelberg, 2008, pp. 508-511.
- [5] G. Hickman, J. Krolik, Non-recurrent wideband continuous active sonar, in *proceedings IEEE OCEANS 2012*, Hampton Roads, VA, October 2012.
- [6] D. Grimmer, Multistatic sensor placement with the complementary use of Doppler sensitive and insensitive waveforms, *NURC Technical Report SR-427*, July 2005.
- [7] S. Nardone, V. Aidala, Observability Criteria For Bearings-Only Target Motion Analysis, *IEEE Trans. Aerospace and Electronic Systems*, Vol. AES-17, No. 2, March 1981.
- [8] R. Ricks, C. Wakayama, D. Grimmer, Passive Acoustic Tracking for Cueing a Multistatic Active Acoustic Tracking System, *Proceedings of the MTS/IEEE Oceans '12 Conference*, May, 2012, Yeosu, Korea.
- [9] C. Wakayama, D. Grimmer, R. Ricks, Active Multistatic Track Initiation Cued by Passive Acoustic Detection, in *proceedings 15th International Conference on Information Fusion*, Singapore, July, 2012.
- [10] M. B. Guldogan, D. Lindgren, F. Gustafsson, H. Habberstand, U. Orguner, Multiple target Tracking with Gaussian Mixture PHD Filter using Passive Acoustic Doppler-Only Measurements, in *proceedings 15th International Conference on Information Fusion*, Singapore, July, 2012.
- [11] E. Hanusa, D. Krout, M. Gutpa, Estimation of Position from Multistatic Doppler Measurements, in *proceedings 13th International Conference on Information Fusion*, Edinburgh Scotland, July, 2010.
- [12] L. D. Stone, C. A. Barlow, T. Corwin, Bayesian Multiple Target Tracking, Artech House, Inc, Norwood, MA, 1999.
- [13] R. Streit, B. Osborn, K. Orlov, Hybrid Intensity and Likelihood Ratio Tracking (iLRT) Filter for Multitarget Detection, in *proceedings 14th International Conference on Information Fusion*, Chicago, IL, U.S.A., July 2011.
- [14] S. Blackman and R. Popoli, *Design and Analysis of Modern Tracking Systems*, Artech House, Norwood, MA, U.S.A., 1999, Chap. 4, pp. 203-205.
- [15] R. Mahler, "Multi-target Bayes filtering via first-order multi-target moments," *IEEE Trans. AES*, vol. 39, no. 4, pp. 1152-1178, 2003
- [16] B. Vo, W. Ma, "The Gaussian Mixture Probability Hypothesis Density Filter", *IEEE Trans. Signal Processing*, Vol. 54, No. 11, pp. 4091-4104, November 2006.
- [17] K. Panta, B. Vo, S. Singh, and A. Doucet, Probability Hypothesis Density filter versus multiple hypothesis tracking, in *proceedings Signal Processing, Sensor Fusion and Target Recognition XIII, SPIE*, vol. 5429, pp. 284-295, 2004.
- [18] D. Grimmer, C. Wakayama, R. Ricks, Simulation of Passive and Multistatic Active Sonar Contacts, in *Proceedings of the 4th International Conference on Underwater Acoustic Measurements Technologies and Results*, June, 2011, Kos, Greece.